

# Spin-polarized current oscillations in diluted magnetic semiconductor multiple quantum wells

Manuel Béjar,<sup>1</sup> David Sánchez,<sup>1,2</sup> Gloria Platero,<sup>1</sup> and A.H. MacDonald<sup>3</sup>

<sup>1</sup>*Instituto de Ciencia de Materiales de Madrid (CSIC), Cantoblanco, 28049 Madrid, Spain*

<sup>2</sup>*Département de Physique Théorique, Université de Genève, CH-1211 Genève 4, Switzerland*

<sup>3</sup>*Department of Physics, The University of Texas at Austin, Austin, Texas 78712*

(Dated: February 1, 2008)

We study the spin and charge dynamics of electrons in n-doped II–VI semiconductor multiple quantum wells when one or more quantum wells are doped with Mn. The interplay between strongly nonlinear inter-well charge transport and the large tunable spin-splitting induced by exchange interactions with spin-polarized Mn ions produces interesting new spin dependent features. The tunneling current between quantum wells can be strongly spin polarized and, under certain conditions, can develop self sustained oscillations under a finite dc voltage. The spin polarization oscillates in both magnetic and nonmagnetic quantum wells and the time average in magnetic wells can differ from its zero-voltage value. Our numerical simulations demonstrate that the amplitude of the spin polarization oscillations depends on the distribution of magnetic wells within the sample. We discuss how the spin polarized current and the spin polarization of the quantum wells can be tailored experimentally.

PACS numbers: 72.25.Dc, 72.25.Mk, 73.21.Cd, 75.50.Pp

## I. INTRODUCTION

Current information technology devices are based on the manipulation of electrical charge flow using electric fields. Recent technological developments<sup>1</sup> that exploit magnetotransport effects in ferromagnetic metals have increased interest in exploring other ideas. Effects based on the electron spin degree of freedom can be used either to improve device functionality, or to create radically new devices that either implement new processing algorithms, as in quantum computing, or that are based on new physical principles, as in spin-FETs.<sup>2</sup> The extreme sensitivity to external magnetic fields<sup>3</sup> that has been exploited in ferromagnetic metals is ultimately a consequence of the collective behavior of many electronic spins that follows from long-range ferromagnetic order. Ferromagnetic semiconductors are important because their magnetic properties can in principle be engineered by doping or by adjusting gate voltages. Considerable progress has been recently made in manipulating the ferromagnetism that occurs in a number of common III–V compound semiconductors when they are doped with the magnetic element Mn.<sup>4,5,6</sup> Although they are not normally ferromagnetic, II–VI semiconductors doped with Mn, also respond strongly to external magnetic fields and have properties<sup>7,8,9</sup> that are similar in many respects. The transport properties of Mn-based heterostructures have been studied<sup>10</sup> including miniband transport in strongly-coupled superlattices doped with Mn.<sup>11</sup>

In a recent paper<sup>12</sup> three of us analyzed the nonlinear transport properties of II–VI semiconductors with weakly-coupled highly n-doped quantum-wells in which one or more of the quantum wells is doped with Mn. The interplay between electronic spin, charge accumulation, and resonant interwell tunneling effects that takes place in these systems has been shown to alter the formation

of stable electric field domains and to produce hysteretic behavior in both spin and charge distributions. Spin polarization is induced in both magnetic and nonmagnetic quantum wells when driven by strong dc electric fields.

In nonmagnetic highly n-doped semiconductor weakly coupled multiple-quantum-wells, it is well known that dc electrical transport is dominated by the formation of electric field domains. This effect is reflected in the nonlinear current-voltage characteristics<sup>13,14</sup> which present a sawtooth structure that arises from the interplay between electron–electron interactions and resonant inter-subband tunneling between neighboring quantum wells. When the carrier density is below a critical value, however, the formation of electric field domains is not stable and the non linear transport properties change drastically in comparison with the highly n-doped systems. Intermediate n-doped systems have very rich behavior. The time-averaged current–voltage  $J$ – $V$  characteristics presents flat plateaus. Real-time measurements show that within a plateau the current has an undamped oscillatory dependence on time.<sup>15</sup> These self-sustained electronic current oscillations<sup>15,16</sup> come from the dynamics of the domain wall separating electric field domains and persist even at room temperature, making these devices promising candidates for microwave generation<sup>15</sup> with frequencies that extend from kHz to GHz.

In this paper we explore new features that occur in weakly coupled quantum wells *that support self-sustained oscillations* when they are doped with magnetic impurities. In Section II we briefly review the model that we use for incoherent transport between quantum wells which can contain magnetic impurities. In Section III we summarize and discuss the results we have obtained by solving this model numerically for some representative circumstances. Finally, in Section IV we present our conclusions.

## II. MODEL

Our theory of transport through diluted magnetic semiconductor multiple-quantum-wells is built on (i) a theory for the tunneling current between two spin-polarized two-dimensional electron gases (2DEGs); (ii) a continuity equation that accounts for relaxation of nonequilibrium spin populations; (iii) a relationship between the up and down chemical potentials and their densities; (iv) a mean-field theory for the interaction between 2DEG electrons and Mn spins; and (v) an expression to take into account the Coulomb interaction between charge accumulations in the quantum wells.

In weakly coupled multiple-quantum-wells, it is a good approximation to treat tunneling of quasiparticles between neighboring quantum wells by leading order perturbation theory. We ignore interwell spin-flip processes, so that currents are carried between wells by the two spin subsystems in parallel. Accordingly, the current per spin  $\sigma$  from the  $i$ th well to the  $(i+1)$ st well,  $J_{i,i+1}^\sigma$ , can be properly described by a *Transfer Hamiltonian* model<sup>14,17</sup> with a Lorentzian lifetime broadening of each quasiparticle's spectral density. Our Lorentzian halfwidth,  $\gamma = \hbar/\tau_{\text{scatt}}$ , is energy independent, purely phenomenological, and represents the combined effects of interface roughness, phonons, and impurity effects. Spin relaxation processes are not included in  $\gamma$ . The scattering times in quantum wells are shorter than any other time scale of the problem ( $\tau_{\text{scatt}} \simeq 0.1 - 1$  ps); we therefore assume that the electrons in each well reestablish local equilibrium between successive tunneling events and that their temperature is that of the lattice. The exchange interaction that couples  $s$  conduction band electron spins and  $d$  Mn local moments is ferromagnetic<sup>4</sup> and favors parallel alignment of the local moment  $S$  and band electron spins  $s$ :  $\mathcal{H}_{\text{int}}^{sd} = J_{sd} \sum_I \vec{S}_I \cdot \vec{s}(\vec{r}_I)$ , where the sum is extended over the positions  $I$  of the magnetic impurities and  $J_{sd}$  is the exchange integral (which we take as a constant).

When the mean-field and virtual crystal approximations are employed,<sup>18</sup> the effect of the exchange interaction is to make the subband energies spin-dependent in those quantum wells that contain Mn ions:  $E_j^\sigma = E_j - s\Delta$ , where  $\Delta \equiv 2J_{sd}N_{\text{Mn}}SB_S(g\mu_B BS/k_B T_{\text{eff}})$ ,<sup>4</sup> and  $s = +1/2(-1/2)$  for  $\sigma = \uparrow(\downarrow)$ . We must also take into account the microscopic processes that permit the quasiparticle system to bring its spin-subsystems into equilibrium within each quantum well. Slow conduction band spin relaxation<sup>19</sup> makes the effects we discuss stronger and is an important motivation for this study. Relaxation times in excess of 1 ns have been established experimentally<sup>20</sup> in II-VI semiconductor quantum wells without Mn. In II-VI diluted magnetic semiconductor quantum wells these times are reduced to tens of picoseconds (but are still larger than  $\tau_{\text{scatt}}$ ).<sup>21</sup> Fermi's Golden rule leads to the following equations for the spin relax-

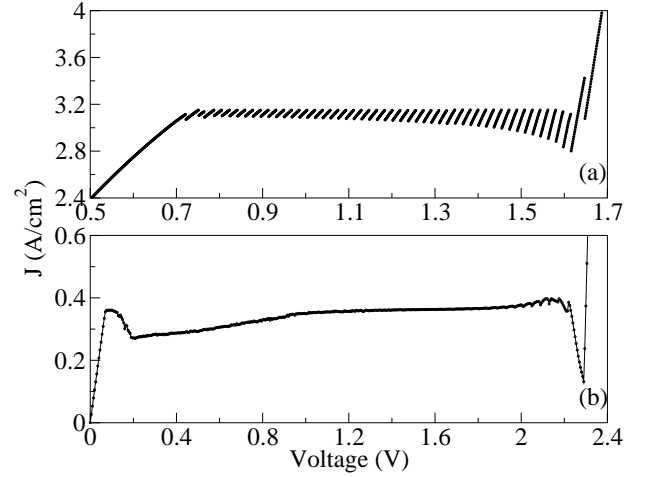


FIG. 1:  $J$ - $V$  curves for a 50-well n-doped 5-nm ZnSe/10-nm Zn<sub>0.8</sub>Cd<sub>0.2</sub>Se system with fractional MnSe monolayers at the 1st and 50th quantum wells. Well doping is (a)  $N_w = 1 \times 10^{12} \text{ cm}^{-2}$  and (b)  $N_w = 9 \times 10^{10} \text{ cm}^{-2}$ . Contact doping is (a)  $N_c = 1.1 \times 10^{12} \text{ cm}^{-2}$  and (b)  $N_c = 9.9 \times 10^{10} \text{ cm}^{-2}$ . Case (a) corresponds to a highly n-doped sample. In that case, the current is stationary and electric field domain formation takes place. It is reflected in the sawtooth-like structure that presents  $J$  versus  $V$ . Case (b) corresponds to an intermediate n-doped sample. In that case, the current presents self-sustained oscillations and the time-averaged current shown in the figure above shows a flat plateau behaviour.

ation rate equation within each well:<sup>22</sup>

$$\frac{dn_i^\sigma}{dt} = -\frac{\mu_i^\sigma - \mu_i^{\bar{\sigma}}}{\tau_{\text{sf}}} \nu_0, \quad (1)$$

where  $\bar{\sigma}$  is the spin opposite to  $\sigma$ ,  $\tau_{\text{sf}}$  is the spin-scattering time,  $\nu_0$  is the two-dimensional density-of-states per spin, and  $n_i^\sigma$  is the spin  $\sigma$  charge density in the  $i$ th-well. For  $\Delta > \mu_i^\uparrow - E_{i1}^\uparrow$ , Eq. (1) must be modified:<sup>12</sup>

$$\frac{dn_i^\downarrow}{dt} = -\frac{n_i^\downarrow}{\tau_{\text{sf}}} = -\frac{\mu_i^\downarrow - E_{i1}^\downarrow}{\tau_{\text{sf}}} \nu_0, \quad (2)$$

$$\frac{dn_i^\uparrow}{dt} = -\frac{dn_i^\downarrow}{dt}. \quad (3)$$

For large enough  $\Delta$ , Eq. (2) leads to an equilibrium state with full spin polarization. The continuity equations that describe the time evolution of the partial densities in each quantum well include both spin-relaxation and transport currents:

$$\frac{dn_i^\sigma}{dt} = \frac{J_{i-1,i}^\sigma - J_{i,i+1}^\sigma}{e} - \frac{\mu_i^\sigma - \mu_i^{\bar{\sigma}}}{\tau_{\text{sf}}} \nu_0 \quad i = 1, \dots, N \quad (4)$$

for the case  $\mu_i^\uparrow - E_{i1}^\uparrow > \Delta$  ( $N$  is the number of quantum wells). Otherwise, Eqs. (2-3) must replace the second term on the right-hand side of Eq. (4).

### III. RESULTS

In order to obtain electric field domain physics it is necessary to account for electron-electron interactions among conduction band electrons at the mean-field level by solving the Poisson equation.<sup>12</sup> Including a displacement current contribution, the total current density  $J(t)$  traversing the sample at time  $t$  is  $J(t) = \epsilon \frac{dV_i}{dt} + J_{i,i+1}(t)$  which is independent of  $i$  and where  $J_{i,i+1}(t) = J_{i,i+1}^\uparrow(t) + J_{i,i+1}^\downarrow(t)$ ,  $\epsilon$  is the sample permittivity,  $d$  is the multiple-quantum well period and  $V_i$  the voltage drop between wells  $i$  and  $i+1$ . We model a  $N = 50$  n-doped ZnSe/Zn<sub>0.8</sub>Cd<sub>0.2</sub>Se multiple-quantum-well system<sup>8</sup> with well and barrier widths 10 nm and 5 nm, respectively. Mn impurities are placed in the 1st and 50th quantum wells. We have chosen the spin relaxation time within the magnetic and nonmagnetic quantum wells to be  $\tau_{sf} = 10^{-11}$  s and  $\tau_{sf} = 10^{-9}$  s, respectively. The quantum wells and the contacts are n-doped with  $N_w$  and  $N_c = \kappa N_w$  respectively. We take  $\kappa = 1.1$ . Figure 1 shows the  $J$ - $V$  characteristics for (a)  $N_w = 1 \times 10^{12} \text{ cm}^{-2}$  and (b)  $N_w = 9 \times 10^{10} \text{ cm}^{-2}$ . The spin splitting is  $\Delta = 2$  meV in both cases. With these parameters, the magnetic quantum wells (if taken as isolated) are partially polarized:  $P = 7\%$  [case (a)] and  $P = 75\%$  [case (b)], where  $P_i = (n_i^\uparrow - n_i^\downarrow)/n_i$  is the spin polarization of the  $i$ th-well. As expected, Fig. 1(a) exhibits a series of sharp discontinuities in the negative differential conductance region which are linked to the formation of static electric field domains. Along each branch, charge accumulates at the domain wall, forming a monopole that jumps discretely toward the emitter as  $V$  increases. When  $N_w$  is lowered [see Fig. 1(b)], the branches are substituted by a plateau on which current oscillates periodically with time. We observe undamped self-oscillations of the current in the range  $V = 0.2$ – $1.5$  V.

In Fig. 2 we plot the total current (a), and the spin-up (b) and spin-down (c) currents toward the collector as a function of time for  $V = 0.5$  V for the sample described in Fig. 1(b), i.e., for an intermediated n-doped sample:  $N_w = 9 \times 10^{10}$  and  $N_c = 9.9 \times 10^{10}$  which presents self sustained oscillations in the absence of magnetic quantum wells. The current oscillations have a period of the order of  $5 \mu\text{s}$ , i.e., with a frequency in the kHz range. We observe an irregular shape for the current amplitude in all the three cases. The current spikes that are superimposed on the main periodic structure reflect discrete jumps of a domain wall separating electric field domains from well to well.<sup>16</sup> The current oscillations emerge from the dynamics of the domain wall which usually consists of a charge accumulation layer (monopole) spread over one or two quantum wells. In nonmagnetic multiple-quantum-wells the dynamics of the monopole has been theoretically described and experimentally observed.<sup>15</sup> Lowering the contact charge doping, the domain walls lead to traveling dipoles<sup>23</sup> that consist of one accumulation and one depletion charge layer located in separated quantum wells and

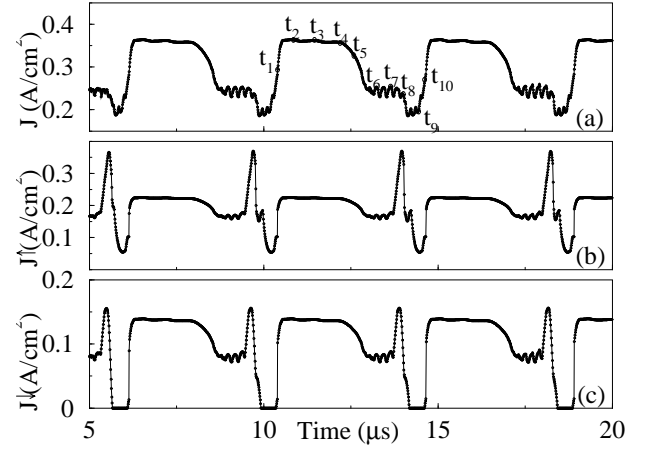


FIG. 2: (a) Total time-dependent current (tunneling+displacement), (b) spin-up, and (c) spin-down time-dependent current at a fixed dc bias voltage  $V_{dc} = 0.5$  V for the superlattice described in Fig. 1(b). The current oscillations present a flat region and overimposed spikes (see the text below). Comparison of (b) and (c) indicates that the current towards the collector is partially spin-up polarized.

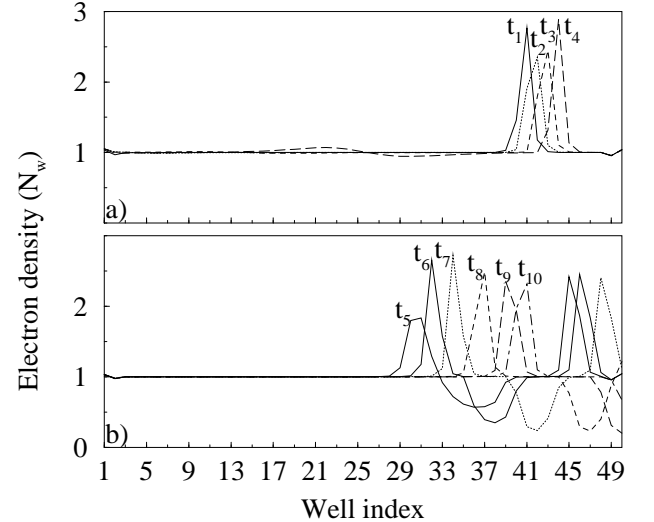


FIG. 3: Local distribution of the electron density through the sample at fixed dc bias voltage:  $V_{dc} = 0.5$  V for the different times marked in Fig. 2(a). At the flat region of the oscillation in Fig. 2(a) the domain wall consists of one charge accumulation layer (monopole) which propagates just within a small part of the superlattice. With increasing time ( $t_5 - t_{10}$ ) the domain wall configuration changes and it becomes a dipole (one charge accumulation and one charge depletion layer) which runs through half of the superlattice.

have distinct dynamics. (The dipole charge front wave is similar to the one responsible of the Gunn effect in bulk semiconductors). In semiconductor multiple-quantum-wells, monopole and dipole domain walls can coexist at a fixed dc bias<sup>16</sup> under certain conditions.

In Fig. 3(a) we plot the charge density quantum well

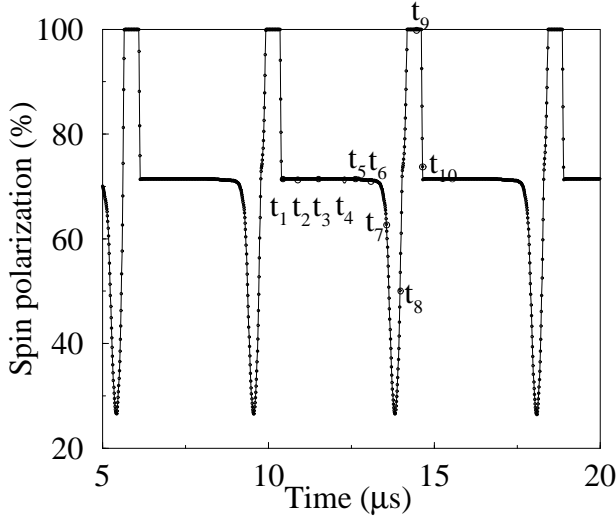


FIG. 4: Spin polarization,  $P$ , in the quantum well closest to the collector as a function of  $t$  for  $V_{DC} = 0.5$  V. The fractional polarization of the isolated quantum well is  $P = 75\%$ . Within the superlattice, in the strongly nonlinear regime, the polarization oscillates and reaches, for a small time window of the period, full spin-up polarization.

distribution at the times  $t_1$ – $t_5$  marked in Fig 2. We observe that for the case illustrated the domain wall is a monopole which travels through only a part of the structure. In Fig. 3(b) the charge density at times  $t_5$ – $t_{10}$  is presented. These plots illustrate an interesting feature of our results: the domain wall is now a dipole with both charge accumulation and depletion. During each oscillation period the domain wall undergoes a transition from a monopole to a dipole one and back. An exciting consequence of this behavior is shown in Fig. 4 where the polarization in the magnetic quantum well is plotted as a function of  $t$ . We observe that the polarization reaches three different values during one oscillation: during the intervals of dipole propagation the polarization abruptly drops and increases up to a practically fully polarization configuration. When the domain wall becomes a monopole the polarization remains practically constant up to the time where the dipole is formed. The constant value of the polarization is close to the value of the polarization of the isolated quantum well.

The previous observation can be explained by looking at how the spin polarization in the Mn-doped quantum well influences the tunneling probability to neighboring wells and by the strongly nonlinear transport in the negative differential conductance region. The chemical potentials for spin up and down electrons within a magnetic quantum well do not take on the same value in the stationary limit as they would do in an isolated quantum well because of the finite spin-flip and tunneling rates and because self-consistency changes the charge density in the quantum wells.

The magnetic quantum well spin-polarization in the

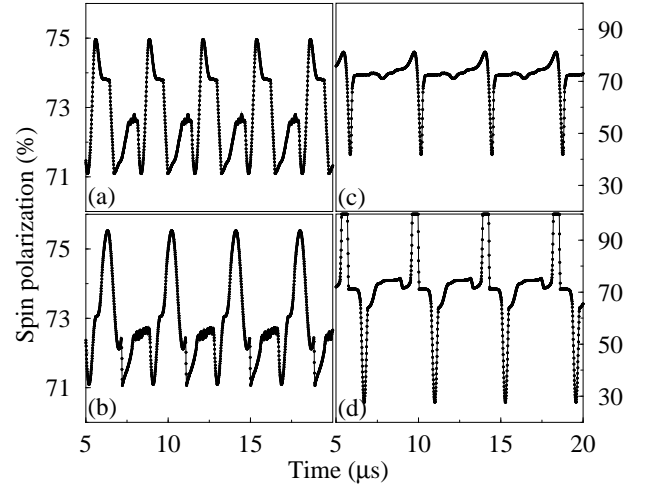


FIG. 5: Spin polarization of the magnetic quantum well, located in the 10th (a), 20th (b), 30th (c), and 40th (d) position at a fixed dc bias,  $V_{dc} = 0.5$  V. In all four cases a second magnetic quantum well is placed at the location closest to the emitter. The polarization corresponding to the isolated magnetic well is  $P = 75\%$ . The depletion charge of the dipole domain wall is centered around the 40th well. This depletion is responsible for the enlargement of the spin polarization and can lead to full polarization [see (d)].

nonequilibrium case may be related to the instantaneous local chemical potentials for majority and minority spins:

$$P = \frac{\nu_0 \Delta}{n_m} + \frac{\delta \mu_m \nu_0}{n_m}, \quad (5)$$

where  $\delta \mu_m = \mu_m^\uparrow - \mu_m^\downarrow$ . This expression is obtained assuming the linear non-interacting 2DEG relationship between density and chemical potential, so that correlation effects are not included:<sup>24</sup>  $n_i^\sigma = \nu_0(\mu_i^\sigma - E_{i1}^\sigma)$ . The above expression for the polarization  $P$  is also valid for non magnetic quantum wells. In this case, the spin splitting is very small and it is basically the second term of Eq. (5) that is responsible for the induced finite polarization.

As we can see from Eq. (5), increasing the density reduces the relative polarization. It follows that a monopole domain wall accumulation layer in the magnetic well will reduce  $P$  compared to the equilibrium case. This reduction was observed for multiple-quantum-wells with stable electric field domains and stationary<sup>12</sup> currents. In contrast, in the self-sustained current oscillations the magnetic well polarization can increase with respect to the isolated case, even reaching full spin-polarization. Comparing Figs. 3 and 4, we note that the high polarization configuration state occurs at  $t = t_9$ , when the front wave is a dipole with one depletion and one accumulation layer (domain walls) and the depletion region is located at the magnetically doped quantum well. The large polarization occurs in part because of the local instantaneous decrease in the total density of electrons in the magnetic well. The frequency, amplitude and shape of the current oscillations depend on the dynamics of the

polarized charge, which itself depends on the distribution of magnetic quantum wells in the sample. Then tailoring the sample configuration should enable control of not only the frequency and amplitude of the current oscillations, but also of the spin polarization and its time dependence. To illustrate this we present in Fig. 5 results for the case in which two magnetic quantum wells are placed in the system, one adjacent to the emitter and another at a variable position. We observe that when the magnetic quantum well is close to the position of the domain wall the amplitude of the polarization oscillations increases [Fig. 5(d)]. Because the polarization depends on the inverse of the charge density, whenever the domain wall enters and leaves the magnetic quantum well, the amplitude of the magnetization oscillations increases and  $P$  oscillates between 20% and 100%. As the magnetic quantum well comes closer to the collector, the polarization exhibits two flat regions within an oscillation. Since the period of these electric field domain oscillations is of the order of 5  $\mu$ s, time resolved measurements of PL in illuminated multiple quantum well samples should allow this polarization change to be observable.

#### IV. CONCLUSION

In closing, we have studied the spin dynamics in multiple-quantum-well systems doped with magnetic im-

purities. We predict time-dependent periodic oscillations of the spin polarized current and of the spin polarization in both magnetic and nonmagnetic quantum wells. The interplay between nonlinearity of the current-voltage relationship and the exchange interaction produces new spin dependent features which are sensitive to spin relaxation times and to the equilibrium exchange fields in the quantum wells which can be tailored by adjusting external field and temperature. These new spin dependent features can potentially be exploited for device applications. In particular, our results for the oscillating spin polarized currents at the collector suggest that these systems could be designed as spin-polarized current injection oscillators.

#### Acknowledgments

This work was supported by the Spanish DGES Grant No. MAT2002-02465, by the European Union TMR Contract FMRX-CT98-0180 and by the European Community's Human Potential Programme under contract HPRN-CT-2000-00144, Nanoscale Dynamics. M. B. acknowledges the MECO for a national grant. Research at the University of Texas was supported by the Welch Foundation and by the Department of Energy under grant DE-FG03-02ER45958.

- 
- <sup>1</sup> G.A. Prinz, Science **282**, 1660 (1998); P. Ball, Nature **404**, 918 (2001); S.A. Wolf, D.D. Awschalom, R.A. Buhrman, J.M. Daughton, S. von Molnár, M.L. Roukes, A.Y. Chtchelkanova, and D.M. Treger, Science **294**, 1488 (2001).
  - <sup>2</sup> S. Datta and B. Das, Appl. Phys. Lett. **56**, 665 (1990).
  - <sup>3</sup> M.N. Baibich, J.M. Broto, A. Fert, F. Nguyen Van Dau, F. Petroff, P. Eitenne, G. Creuzet, A. Friederich, and J.C. Chazelas, Phys. Rev. Lett. **61**, 2472 (1988); G. Binash, P. Grünberg, F. Saurenbach, and W. Zinn, Phys. Rev. B **39**, 4828 (1989).
  - <sup>4</sup> J.K. Furdyna and J. Kossut, in Vol. 25 of *Semiconductor and Semimetals* (Academic Press, New York, 1988); T. Dietl, J. Appl. Phys. **89**, 7437 (2001); B. Lee, T. Jungwirth, and A.H. MacDonald, Semicond. Sci. Technol. **17**, 393 (2002).
  - <sup>5</sup> H. Ohno, J. Magn. Magn. Mater. **200**, 110 (1999).
  - <sup>6</sup> H. Ohno, D. Chiba, F. Matsukura, T. Omiya, E. Abe, T. Dietl, Y. Ohno, and K. Ohtani Nature **408**, 944 (2000).
  - <sup>7</sup> I.P. Smorchkova, N. Samarth, J.M. Kikkawa, and D.D. Awschalom, Phys. Rev. Lett. **78**, 3571 (1997).
  - <sup>8</sup> J.J. Berry, R. Knobel, O. Ray, W. Peoples, and N. Samarth, J. Vac. Sci. Technol. B **18**, 1692 (2000).
  - <sup>9</sup> D. Ferrand, A. Wasiela, S. Tatarenko, J. Cibert, G. Richter, P. Grabs, G. Schmidt, L.W. Molenkamp, and T. Dietl, Solid State Commun. **119**, 237 (2001).
  - <sup>10</sup> J.C. Egues, Phys. Rev. Lett. **80**, 4578 (1998); R. Wessel and I.D. Vagner, Superlatt. and Microstruct. **8**, 443 (1990).
  - <sup>11</sup> M. von Ortenberg, Phys. Rev. Lett. **49**, 1041 (1982); K. Chang, J.B. Xia, and F.M. Peeters, Phys. Rev. B, **65**, 155211 (2002).
  - <sup>12</sup> D. Sánchez, A. H. MacDonald, and G. Platero, Phys. Rev. B **65**, 035301 (2002).
  - <sup>13</sup> L.L. Bonilla, J. Phys.: Condens. Matter **14**, R341 (2002); A. Wacker, Phys. Rep. **357**, 1 (2002).
  - <sup>14</sup> R. Aguado, G. Platero, M. Moscoso, and L.L. Bonilla, Phys. Rev. B **55**, R16053 (1997).
  - <sup>15</sup> J. Kastrup, H.T. Grahn, R. Hey, K. Ploog, L.L. Bonilla, M. Kindelan, M. Moscoso, A. Wacker and J. Galán, Phys. Rev. B **55**, 2476 (1997).
  - <sup>16</sup> D. Sánchez, M. Moscoso, L. L. Bonilla, G. Platero and R. Aguado, Phys. Rev. B **60**, 4489 (1999).
  - <sup>17</sup> J. Bardeen, Phys. Rev. Lett. **6**, 57 (1961).
  - <sup>18</sup> J.K. Furdyna, J. Appl. Phys. **64**, 29 (1988).
  - <sup>19</sup> M.E. Flatté and J.M. Byers, Phys. Rev. Lett. **84**, 4220 (2000).
  - <sup>20</sup> J.M. Kikkawa, I.P. Smorchkova, N. Samarth, and D.D. Awschalom, Science **281**, 1284 (1997).
  - <sup>21</sup> G. Bastard and L.L. Chang, Phys. Rev. B **41**, 7899 (1990); J.C. Egues and J.W. Wilkins, Phys. Rev. B **58**, R16012 (1998).
  - <sup>22</sup> A.H. MacDonald, Phys. Rev. Lett. **83**, 3262 (1999).
  - <sup>23</sup> M. Büttiker and H. Thomas, Z. Phys. B **34**, 301 (1979).
  - <sup>24</sup> A. H. MacDonald in *Dynamical Aspects of Mesoscopic Systems*, Procc. of the XVI Sitges Conference. Eds. D. Reguero, G. Platero, L.L. Bonilla and J. M. Rubi, Springer Verlag, Berlin, (2000).